



OPEN

DATA DESCRIPTOR

Seismic resilience of urban networks: dataset for infrastructure visualization and vulnerability assessment

Marco Civera¹, Fabrizio Aloschi²✉, Galilea Margherita Di Maio¹, Juan Pablo Fierro Carrasco¹, Andrea Miano³, Bernardino Chiaia¹ & Andrea Prota²

We provide geographic information system (GIS) data and a multimodal dataset from a systematic infrastructure vulnerability assessment in the urban road networks of Turin and Naples, Italy. The seismic typologies of the relevant structural objects (SOs), including bridges, buildings, and roads, were evaluated using digital elevation models (DEMs) and satellite data. The presented GIS data are essential for visualizing and spatially interconnecting SOs; this enables network modeling as a complex system within the Spatial Data Infrastructure (SDI) portfolio of interest. The dataset also includes landslide characteristics from Geoportale Piemonte and the GeoNetwork catalog. Potential applications include resilience analysis, seismic risk assessment, emergency response planning, and post-disaster recovery estimations. Moreover, the dataset helps investigate the interplay between structural vulnerability and geohazards like landslides, heavy rainfall, and earthquakes. Notably, it is particularly relevant for research on urban networks as complex systems, where SDIs assess transportation efficiency and functionality in both pre- and post-event scenarios.

Background & Summary

Resilience is defined and evaluated across a wide range of disciplines, including material science, sociology, biology, ecology, and engineering. In the field of engineering, it assesses how a system responds to perturbations caused by external factors, with key investigations focusing on the impact of such perturbations on communities¹. The strong link between community resilience and the resilience of its critical infrastructure is undeniable, thus driving extensive research in this direction^{2,3}. Along these lines, resilience can be defined as a quantitative and qualitative measure of an engineering system's preparedness to recover from damage^{4,5} that applies also to multi-hazard contexts⁶. As communities rely on cities' core functions, numerous researchers have conducted resilience assessments of lifeline systems, proposing new frameworks for water networks, power systems, and other critical infrastructure. Among these frameworks, transportation networks^{7–9} coupled with the structural vulnerability of their components¹⁰, e.g., buildings and bridges^{11–14}, stand out as the most crucial since they underpin the functionality of all other systems. The dataset¹⁵ presented in this paper focuses on this key framework.

In these lines, there is a growing need for information and communication technology (ICT)-based tools to support decision-makers in disaster preparedness and response. Spatial Data Infrastructures (SDIs)¹⁶ play a key role by allowing access to and sharing of multisource geospatial data over the Internet to support disaster risk reduction and emergency planning. However, SDIs still rely on human input for data collection, querying, and analysis, whether from field observers or experts who identify critical environmental conditions. In this context, we share a dataset with strong potential applications in ICT-based tools and SDIs, including i) GIS data of road networks (RNs), ii) seismic vulnerability data of buildings and bridges, and iii) landslide characteristics data. ICT-based systems can employ (i) to optimize vehicle routes and assess traffic disruptions in post-event

¹Department of Structural, Building and Geotechnical Engineering, Politecnico di Torino, Corso Duca degli Abruzzi, 24, 10129, Turin, Italy. ²Department of Structures for Engineering and Architecture, University of Naples "Federico II", Via Claudio 21, 80125, Naples, Italy. ³Department of Engineering, Telematic University Pegaso, Centro Direzionale Isola F2, 80143, Napoli, Italy. ✉e-mail: fabrizio.aloschi@unina.it

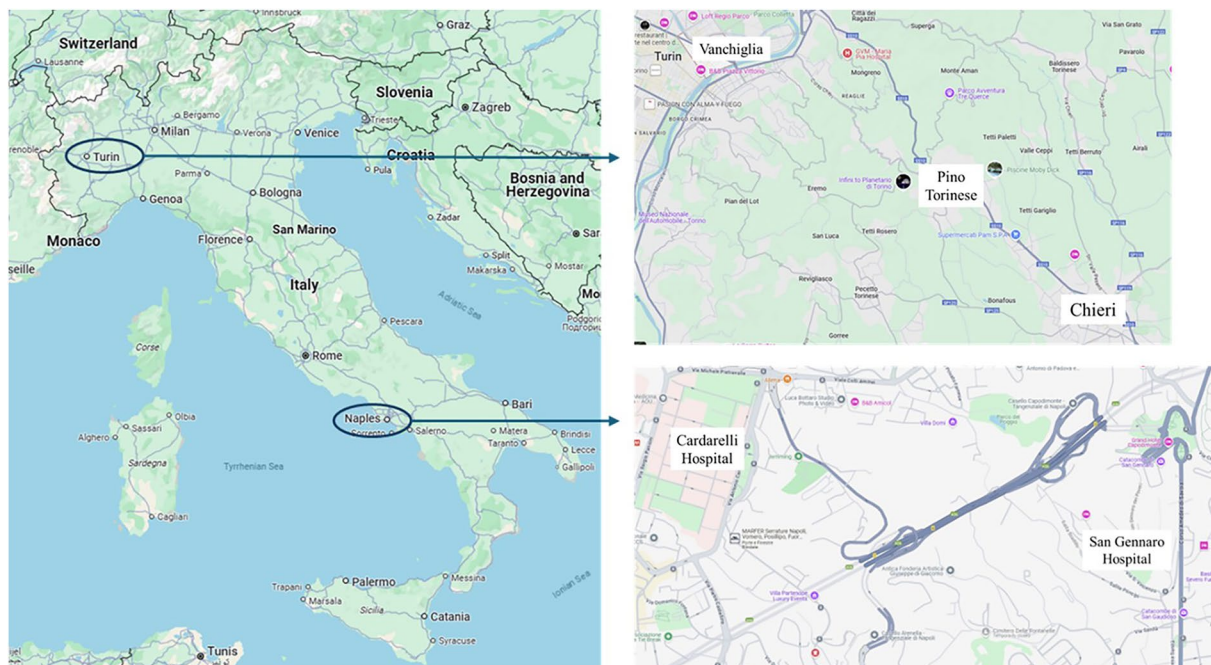


Fig. 1 (a) Map of Italy showing Turin and Naples, and zoom in on the regions of interest for the city of (b) Turin, and (c) Naples.

scenarios resulting from building or bridge damage. Regarding (ii), vulnerability data can support damage prediction models, guide rapid inspection efforts, and inform retrofitting strategies. Finally, (iii) can aid in the development of early warning systems with critical thresholds for each landslide, thereby enabling automated alerts triggered by specific intensity levels of seismic events and rainfall.

Methods

This dataset¹⁵ served some research focused on assessing the seismic and landslide vulnerability of two RNs: one stretch connecting a hospital in Turin (Vanchiglia district) to the city limits of Chieri, passing through the village of Pino Torinese in a hilly countryside, and one connecting two hospitals in Naples, the Cardarelli Hospital and the San Gennaro Hospital, in an urban and densely populated environment, respectively for Turin and Naples, as depicted in Fig. 1.

The dataset¹⁵ is schematically organized as depicted in Fig. 2, as a workflow showing the steps for its creation and content, including case study setup, mapping of roads, structures, and landslides, extraction of attributes, hazard and vulnerability assessments through, respectively, seismic demand, defined in terms of peak ground acceleration, PGA_d , and seismic capacity, namely, PGA_c . The flowchart finally shows data organization.

Each path was selected based on its strategic importance for transportation, proximity to critical infrastructure, and shortest travel distance and time. In particular, for the Turin case study, the last tract from the city limits of Chieri to Chieri Hospital was not considered, as it is identical for all selected paths and does not include critical infrastructures, such as tunnels or bridges. More details can be found in Miano *et al.*¹⁰. Firstly, the routes were selected and spatially mapped on the open source software QGIS¹⁷, i.e., a public project hosted on www.QGIS.org, licensed under GNU GPLv2+. The procedure used for the QGIS project of both case studies is described schematically in Fig. 3. It consisted in identifying the city functions, i.e., the origin-destination (OD) points for the analyses. Specifically, in this study, we used hospitals as ODs. These define the terminals for a series of suitable connecting paths within the road network, and the characterization of potential structural and landslide interferences with the previously defined connecting paths.

Then, geological, seismic, and structural data were collected from online free sources (such as the INGV¹⁸, ISPRA¹⁹, GeoPortale Piemonte²⁰, and GeoPortale Campania²¹ websites) or physical archives. These pieces of information were subsequently georeferenced and added to the database.

Four alternative paths were considered for Turin, as shown in Figs. 4 and 5:

1. SS10 via Traforo del Pino (Pino Nuovo), crossing Ponte Sassi
2. SS10 via Traforo del Pino (Pino Nuovo), crossing Corso Regina Margherita
3. Corso Chieri (Pino Vecchio), crossing Ponte Sassi
4. Corso Chieri (Pino Vecchio), crossing Corso Regina Margherita

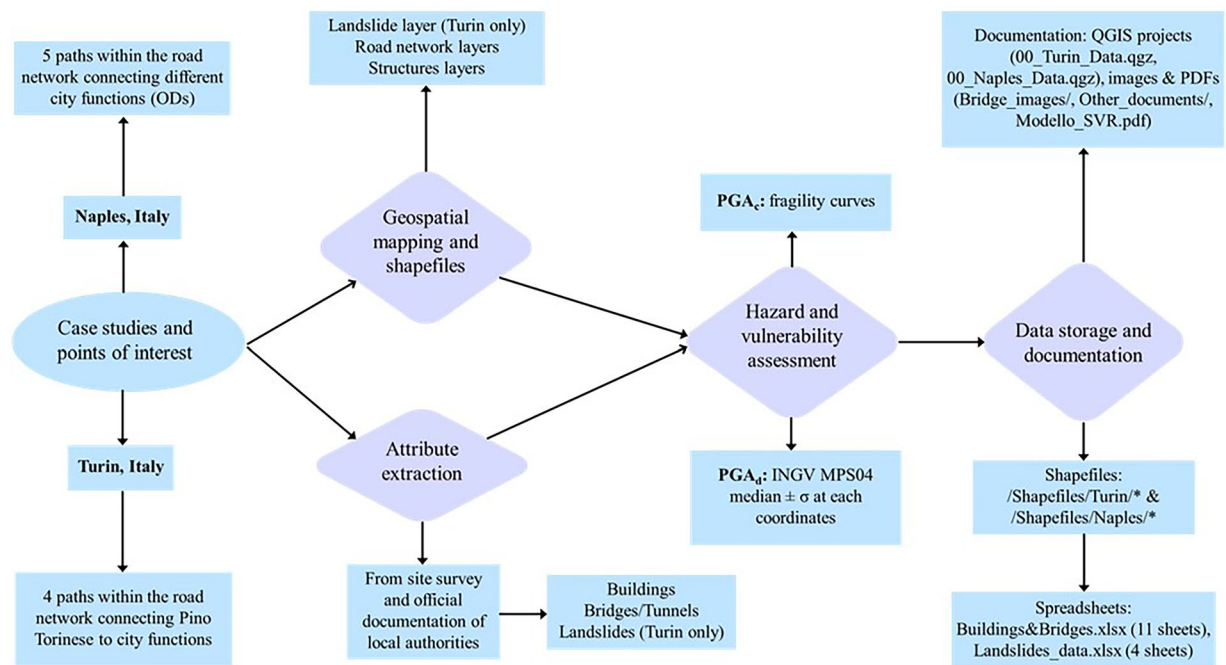


Fig. 2 Flowchart describing the dataset.

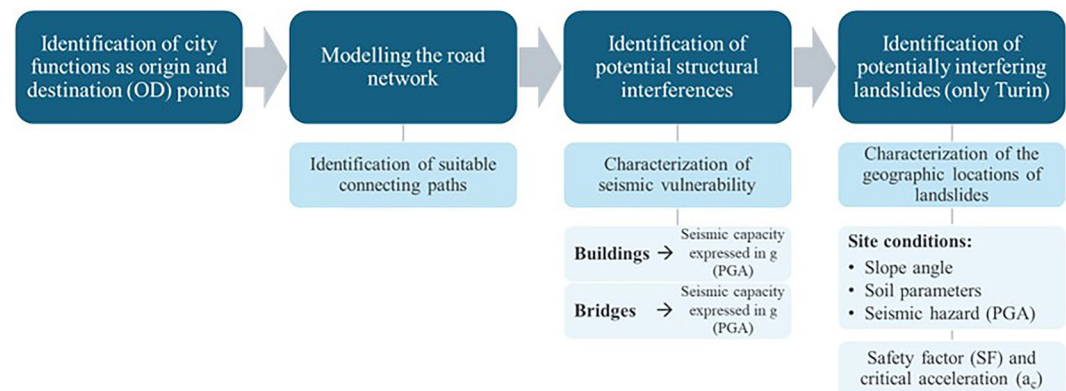


Fig. 3 Flowchart describing the procedure adopted in the QGIS project of the dataset¹⁵.

For Naples, five paths were considered, as depicted in Figs. 6 and 7:

1. URBA 1: Passes through Arenella, connecting to Tangenziale di Napoli.
2. URBA 2: Travels through Colli Aminei and approaches the Policlinico area.
3. TANA 1: Crosses under the Tangenziale di Napoli, near the Zona Ospedaliera connections.
4. TANA 2: Passes through Capodimonte, crossing Via del Poggio
5. TANA 3: crossing the Via Santa Teresa degli Scalzi bridge.

Where the acronym ‘URBA’ stands for urban and ‘TANA’ stands for Tangenziale di Napoli, as these three paths follow the urban A56 highway at some point, while the other two are limited to other regular city roads.

These configurations were analyzed simultaneously, considering the potential risks posed by nearby infrastructure, such as buildings, viaducts, and bridges, under seismic events, as well as assessing slope stability and the effects of rainfall-induced soil saturation.

For this, the dataset¹⁵ design involved two main phases: a qualitative mapping phase using spatial analysis software (the aforementioned QGIS, v3.34.11; <https://qgis.org/>) and a subsequent quantitative analysis phase employing seismic fragility curves.

Preliminary qualitative analysis and data mapping. The initial qualitative phase of the study involved a thorough mapping using QGIS software to organize and visualize the spatial data for the road network. The four paths for Turin and the five for Naples were mapped, including the identification and classification of surrounding

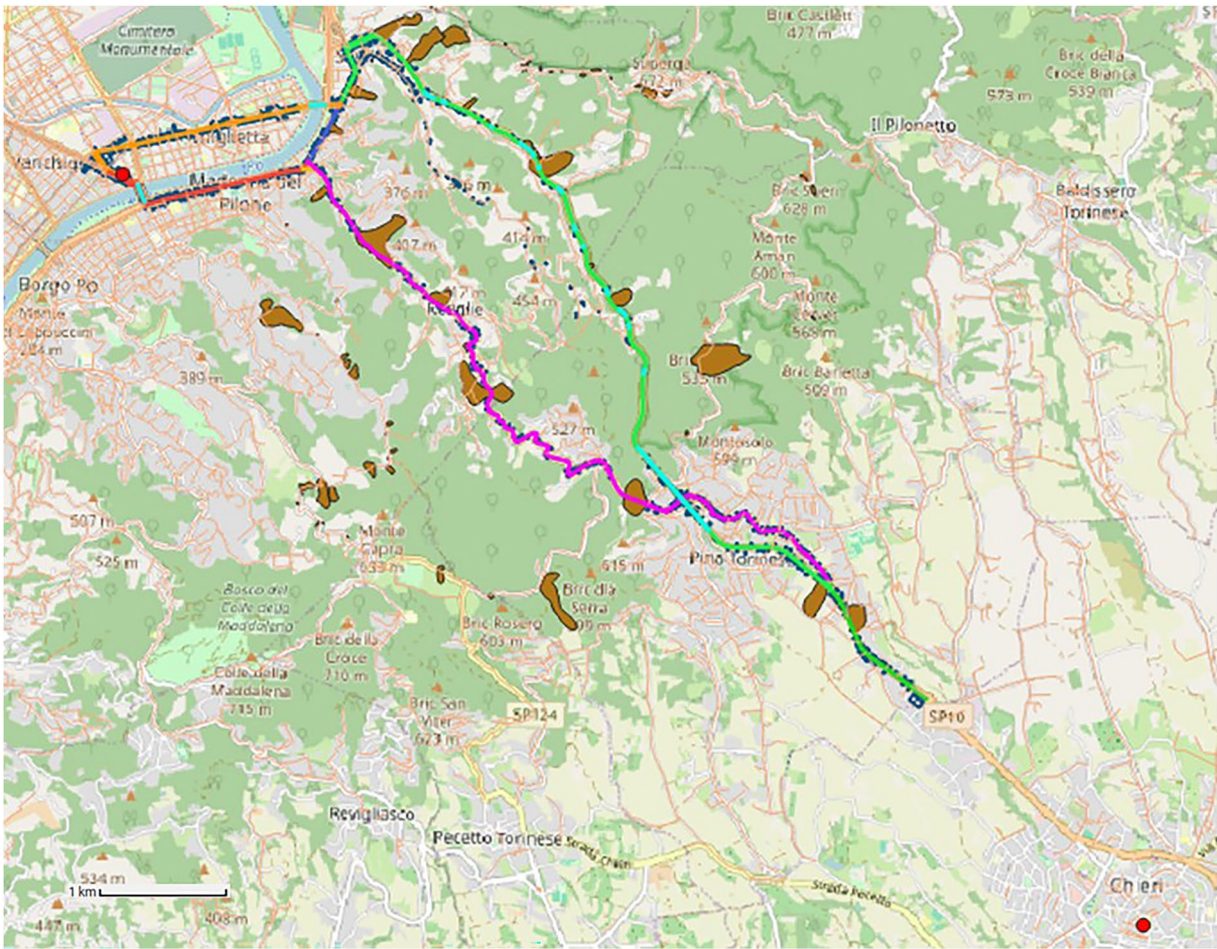


Fig. 4 General overview of Turin’s geospatial data in the GIS software window, showing hospitals (red dots), paths (solid colored lines), buildings (blue dots), major infrastructures (i.e., bridges and tunnels, cyan), and landslides (brown areas). The four paths from (1) to (4) are given by: (1) the concatenation of the green and orange lines; (2) the green, dark blue, and red lines; (3) the purple, dark blue, and orange lines; and (4) the purple and red lines.

| | Height class | θ_{DS1} | θ_{DS2} | θ_{DS3} | θ_{DS4} | θ_{DS5} | β |
|--------------------------|--------------|----------------|----------------|----------------|----------------|----------------|---------|
| Gravity loads | Low | 0.192 | 0.501 | 0.846 | 1.413 | 1.576 | 0.789 |
| | Medium | 0.113 | 0.223 | 0.357 | 0.741 | 0.811 | 0.639 |
| | High | 0.073 | 0.106 | 0.146 | 0.302 | 0.449 | 0.404 |
| Seismic design pre-1981 | Low | 0.316 | 0.565 | 0.810 | 1.109 | 1.698 | 0.682 |
| | Medium | 0.207 | 0.424 | 0.636 | 0.953 | 1.739 | 0.713 |
| | High | 0.186 | 0.306 | 0.423 | 0.687 | 1.091 | 0.499 |
| Seismic design post-1981 | Low | 0.422 | 1.163 | 1.822 | 3.024 | 4.458 | 0.951 |
| | Medium | 0.253 | 0.774 | 1.417 | 2.682 | 7.386 | 0.995 |
| | High | 0.183 | 0.351 | 0.598 | 1.129 | 1.196 | 0.531 |

Table 1. Medians (θ) of lognormal distributions of PGA for five Damage States (DSs), and associated standard deviations (β) for reinforced concrete buildings. All PGA measurements are reported in [g].

buildings, viaducts, and the Traforo del Pino tunnel, for the Turin case study. Each structure was cataloged with its own attributes, as discussed in the Data Records section. The geographic coordinates (latitude and longitude) were recorded for each infrastructure point, establishing a spatial dataset within QGIS. For the viaducts, an initial site survey was conducted and later complemented with information from third-party surveys and official documentation from local authorities, wherever available. Figs. 8 and 9 show examples of the initial site surveying, whereas Fig. 10 shows examples of official documentation drawings that were accessed and represent typical transversal and longitudinal cross-sections of the bridge structures along the paths of the Turin case.

| Shapefile (Name of Layer) | Type | #Features | Description | Attribute Name, Description, and Type of Data |
|---------------------------|---------|-----------|---|--|
| Road_Network_To | Line | 4.945 | Road network containing all streets (both considered in the paths of the project and not) in the area of interest | <ul style="list-style-type: none"> - ID (number) - Street name (text) - Paths (text) - Length in meters (number) - Average speed in km/h^a (number) - Free flow speed in km/h^a (number) - Light vehicles per day mean flow^a (number) - Heavy vehicles per day mean flow^a (number) - Total vehicles per day mean flow^a (number) - Road capacity: vehicles per hour^a (number) |
| Buildings_To | Polygon | 817 | Buildings with possible interferences on selected paths in case of seismic overturning | <ul style="list-style-type: none"> - OID (number) - ISTAT identifier (number) - Paths (text) - Height in meters (number) - Floors (text) - Structure (text) - Year of construction (text) - Damage state 1 PGA in g (number) - Damage state 2 PGA in g (number) - Damage state 3 PGA in g (number) - Damage state 4 PGA in g (number) - Damage state 5 PGA in g (number) |
| Landslides_To | Polygon | 81 | Landslides with possible interferences on selected paths in case of earthquake-induced activation | <ul style="list-style-type: none"> - ID (text) - Paths (text) - Type (text) - Slope angle in degrees (number) - Friction angle in degrees (number) - Cohesion in kPa (number) - Soil density in kN/m³ (number) |
| Bridges_Tunnels_To | Line | 16 | Bridges and tunnels along selected paths | <ul style="list-style-type: none"> - ID (number) - Type (text) - Name (text) - Paths (text) - Serviceability limit state PGA in g (number) - Ultimate limit state PGA in g (number) - Number of spans (number) - Length in meters (number) - Commune (text) |
| Points_Interest_To | Point | 2 | Selected points of interest for the case study | <ul style="list-style-type: none"> - ID (number) - Type (text) - Name (text) - Commune (text) - Street name (text) - Civic number (number) - Postal code (number) |

Table 2. Organization of shapefiles and layers for the Turin case study. ^aStatistical data regarding traffic corresponds to that published by “Supervisore Regionale del Traffico” of the Piedmont Region for the year 2023, URL: https://inspire-geoportal.ec.europa.eu/srv/api/records/r_piemon:3dab7c27-ca3e-4dc7-ad7e-9ecef6b9dc9 last accessed 3rd March 2025.

To complete the mapping for the Turin case study, since the paths go through rural areas too, landslide-prone areas were identified using datasets from Geoportale ARPA Piemonte (<https://geoportale.arpa.piemonte.it/app/public/>), the national IFFI landslide database (<https://www.progettoifi.isprambiente.it/>), and the ISPRA IdroGeo landslide database (<https://idrogeo.isprambiente.it/app/>). These datasets provided a detailed list of past landslide events, including coordinates and geotechnical attributes of the soil, which were integrated into the shapefiles and spreadsheets. Additionally, a Digital Elevation Model (DEM) was imported to compute slope angles along each road segment, identifying regions with critical angles that increase the likelihood of landslides. For the Naples case study landslides were omitted, since the paths are in an urban environment not subject to landslide hazard.

Quantitative analysis using seismic fragility curves. Following the preceding qualitative phase, a quantitative analysis was performed to assess seismic vulnerability, and thus, it is worth introducing seismic risk in the context of the two Italian case studies. Risk is usually defined as the probability of loss at a specific location, and it results from the convolution of three parameters: seismic hazard, exposure, and vulnerability. Exposure is typically modeled from building census data, while seismic hazard is expressed through ground-motion parameters, such as the peak ground acceleration (PGA), correlated with damage levels via vulnerability functions. Extensive research has focused on the development of seismic risk maps for Italy, which were thoroughly analyzed and compared in an interesting study by Crowley *et al.*²². Italy ranks among the Mediterranean’s most seismically active regions due to its location at the convergence of the African and Eurasian plates. High seismicity is concentrated in central and southern regions along the Apennine chain, as well as in Calabria and the island of Sicily, and parts of northern Italy, including Friuli, portions of Veneto, and western Liguria. For this reason, regional governments in Italy, responsible for seismic classification, have categorized municipalities into four zones based on seismic hazard, defined by peak ground acceleration (a_g) on rock sites, as follows:

| Shapefile | Type | #Features | Description | Attribute name, description, and type of data |
|---------------------|---------|-----------|--|--|
| Paths_Nap | Line | 144 | Selected paths in the area of interest | <ul style="list-style-type: none"> - ID (number) - Street name (text) - Paths (text) - Length in meters (number) - Maximum speed in km/h (number) |
| Buildings_Nap | Polygon | 425 | Buildings with possible effect on selected paths | <ul style="list-style-type: none"> - OID (number) - Paths (text)^a - Height in meters (number) - Floors (number) - Structure (text) - Damage state 1 PGA in g (number) - Damage state 2 PGA in g (number) - Damage state 3 PGA in g (number) - Damage state 4 PGA in g (number) - Damage state 5 PGA in g (number) |
| Bridges_Nap | Line | 9 | Bridges and overpasses along selected paths | <ul style="list-style-type: none"> - ID (number) - Type (text) - Name (text) - Paths (text) - Serviceability limit state PGA in g (number) - Ultimate limit state PGA in g (number) - Number of spans (number) - Length in meters (number) - Commune (text) |
| Points_Interest_Nap | Point | 2 | Selected points of interest for the case study | <ul style="list-style-type: none"> - ID (number) - Type (text) - Name (text) - Commune (text) - Street name (text) - Civic number (number) - Postal code (number) |

Table 3. Organization of shapefiles and layers for the Naples case study. ^aOut of the five identified paths, the buildings along the path “Urba 1” have not been identified in the GIS representation.

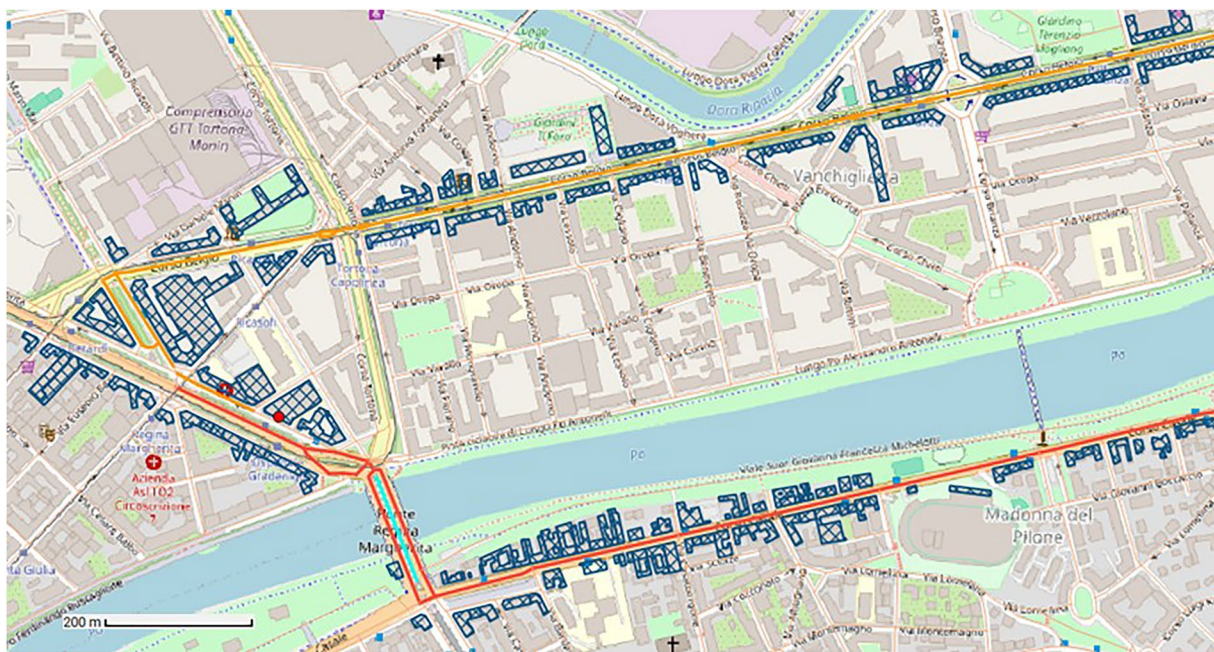


Fig. 5 Zoomed-in view of the GIS software window for the Turin case study, showing the building's footprint with contour and hatch in blue.

Zone 1: Highest hazard, high probability of strong earthquakes ($0.25 < a_g \leq 0.35$ g);
 Zone 2: Significant hazard, strong earthquakes possible ($0.15 < a_g \leq 0.25$ g);
 Zone 3: Moderate hazard, lower likelihood of strong events ($0.05 < a_g \leq 0.15$ g);
 Zone 4: Low hazard, very low probability of significant earthquakes ($a_g \leq 0.05$ g).

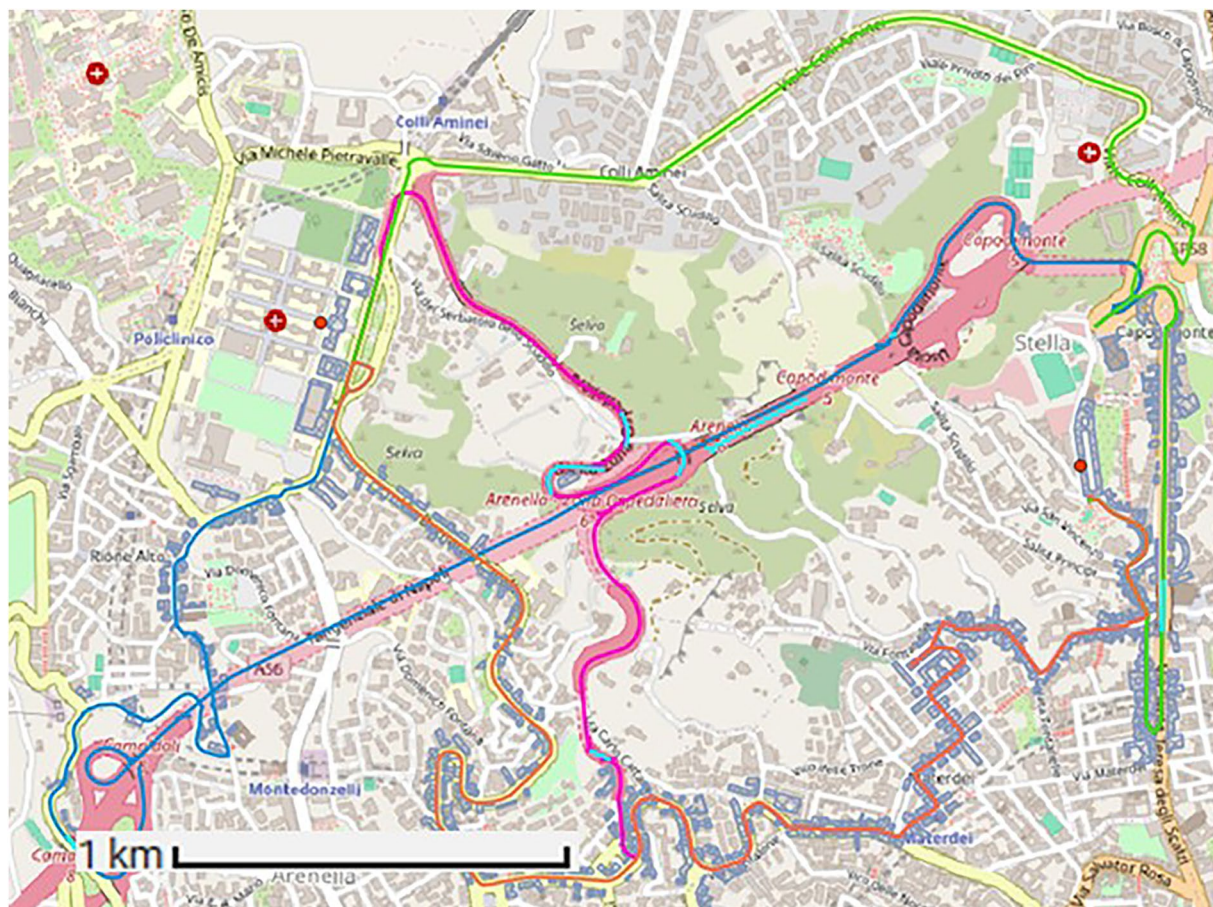


Fig. 6 General overview of Naples' geospatial data in the GIS software window, showing hospitals (red dots), paths (solid colored lines), and buildings (blue polygons). The five paths from (1) to (5) are given by the concatenation of (1) the green, magenta, blue, green, and orange lines; (2) the green, magenta, and orange lines; (3) the blue, green, and orange lines; (4) the green and orange lines; and (5) the orange line.

The city of Naples is classified in Zone 2, with a moderate-to-high seismic hazard, while Turin has lower seismicity and was reclassified from Zone 4 to Zone 3 in 2019.

This data paper aims to present a dataset¹⁵ for infrastructure visualization and vulnerability assessment. Vulnerability, a crucial component of seismic risk, quantifies the susceptibility of structures to earthquake damage. Various models for vulnerability assessment have been developed globally, particularly in the USA²³, in China²⁴, and in Europe²⁵. Notably, Mediterranean countries exhibit similar seismicity, with significant progress in vulnerability modeling recently achieved also in the Balkan region²⁶.

Quantitatively, vulnerability is frequently expressed through fragility curves, which represent the probability of exceeding specific damage states (DS) given an intensity measure (IM). The dataset associated with this paper provides the necessary inputs to evaluate infrastructure vulnerability using fragility curves calibrated for PGA.

In the context of the seismic vulnerability assessment, we calculate two critical parameters:

- The PGA_d (demand Peak Ground Acceleration), which indicates the expected seismic acceleration in the area during an earthquake with a 475-year return period (i.e., a strong quake that statistically happens once every 475 years). To calculate these values, the model MPS04 from the Istituto Nazionale di Geofisica e Vulcanologia (INGV, <https://esse1-gis.mi.ingv.it/>) was used. By entering the exact location (latitude and longitude), the results obtained are three values (for the 16th, 50th, and 84th percentiles). These numbers represent the possible range of shaking intensity at each site, from the least intense (16th percentile) to the most intense (84th percentile). Then, based on the 50th percentile value (median) and the standard deviation of the data, a random distribution is defined by Miano *et al.*^{10,27} to calculate the PGA_d along the network.
- The PGA_c (capacity Peak Ground Acceleration), which signifies the peak acceleration at which a structure loses its functional capacity, was obtained by using seismic fragility curves. These curves provide the structures' seismic thresholds for various damage states. In this dataset¹⁵, two states were considered: the *ultimate limit state* ("SLV") and the *serviceability limit state* ("SLD"). Similar to the calculation of PGA_d , the values of the 50th percentile (median) and standard deviation, described in the following section, have been used to calculate the values of SLV and SLD for each structure through a random distribution defined by Miano *et al.*^{10,27}. Building heights, materials, and construction periods were considered for characterizing buildings

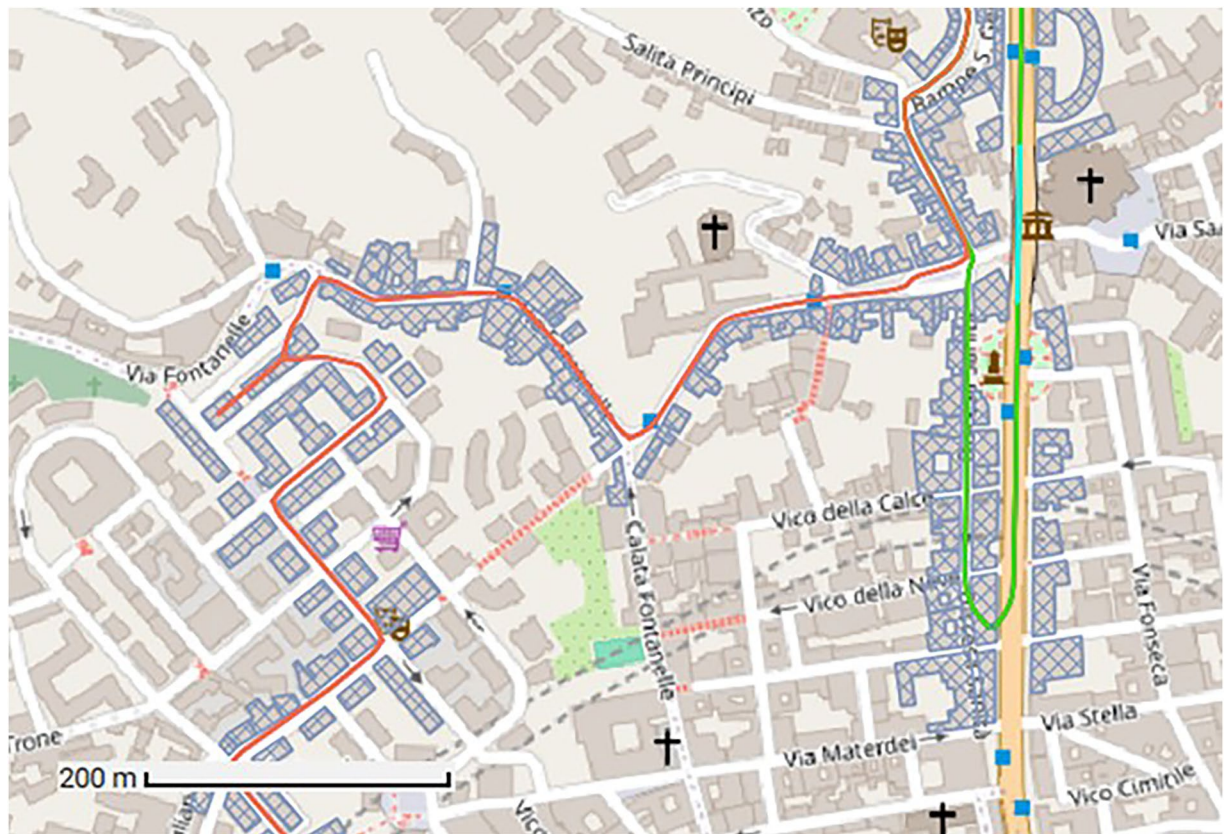


Fig. 7 Zoomed-in view of the GIS software window for the Naples case study, showing the building's footprint with contour and hatch in blue.

and identifying their PGA_c based on previous studies. Similarly, for bridges, the length and spans of bridges were used to distinguish them and associate them with bridges from previous studies for PGA_c definition.

Regarding PGA_c , the estimation of fragility curves was made using MATLAB for curve interpolation and QGIS for spatial data integration. For each viaduct, additional field data, such as the number of spans, pile count, static scheme, and deck type, were gathered during site inspections, enhancing the accuracy of the fragility curves applied.

Given that the viaducts considered in this dataset resembled the characteristics of the Siatista Bridge described in the study of Moschonas *et al.*¹³, the Siatista's fragility curve, reproduced in Fig. 11, was used as a baseline for analysis.

From this curve, SLV values were identified by taking the 50% probability of these thresholds for the *extensive damage* (ultimate limit state) at 0.465 g. For SLD values, the mean of *slight* and *moderate damage* (serviceability limit state) was taken at 0.193 g. Additional fragility curve data were sourced from Nielson²⁸, which categorizes viaducts based on construction material and span count. Most viaducts in this dataset are concrete, three-span structures. Median values for both extensive damage and slight to moderate damage were drawn from the findings of Nielson²⁸. For viaducts with six or more spans, fragility data were obtained from Cardone *et al.*¹⁴ on multi-span simply supported deck bridges. The SLV and SLD values from this study were applied to the corresponding rows in the spreadsheet and shapefiles.

For buildings, empirical fragility curves were applied, differentiating seismic capacity based on structural material (reinforced concrete or unreinforced masonry). Specifically, these were retrieved from studies by Rost *et al.* for buildings made of unreinforced masonry¹¹ and reinforced concrete¹². According to the set of curves specified in these two works, the buildings were further differentiated based on their construction period (with special emphasis on those built before 1981, as they do not adhere to current seismic codes) and height.

Please note that structural material classification was not always available; therefore, the reference papers by Miano *et al.*^{10,27} have performed the studies assuming that the buildings for which material identification has not been possible are made of reinforced concrete.

The probability thresholds for PGA_c (SLD and SLV) were defined based on the fragility curve values of PGA_c that correspond to different seismic damage states. This is reported as an example for reinforced concrete residential buildings in Table 1, where the values reported in the table indicate the medians and standard deviation of lognormal distributions of PGA_c for different damage states (DS1 to DS5) empirically associated with buildings by Rosti *et al.*¹², as derived from hazard maps introduced by INGV¹⁸.

| | |
|------------------------------|---|
| Subject | Civil and Structural Engineering |
| Specific subject area | Efficiency assessment of urban and rural road networks based on physical vulnerability to seismic and landslide events |
| Type of data | Vector network, Spreadsheets, Processed tables, Graph, Raw Figures, Raw Images |
| Data collection | For the Turin case study, road network shapefiles and landslide data were downloaded from the Geoportale Piemonte website. The seismic hazard of the area was obtained from the Italian National Institute of Geophysics and Vulcanology (INGV) website. The landslide hazard was obtained from the Istituto Superiore per la Protezione e la Ricerca Ambientale (ISPRA). Fragility curves were obtained from previous research. For bridges and buildings, the attributes were obtained from official surveys performed by a third party, site surveys made by the Authors, satellite-supported investigations, and ISTAT censuses. |
| Data source location | Primary data sources: - Road Network and buildings' location and footprint (Turin) o Institution: Geoportale Piemonte o City/Town/Region: Turin, Piedmont o Country: Italy o URL: https://www.geoportale.piemonte.it/visregpigo/ - Road Network and buildings' location and footprint (Naples) o Institution: Regione Campania o City/Town/Region: Naples, Campania o Country: Italy o URL: https://sit2.regione.campania.it/node - Seismic Site Hazard o Institution: Italian National Institute of Geophysics and Vulcanology (INGV) o City/Town/Region: Turin, Piedmont; Naples, Campania o Country: Italy o URL: https://esse1-gis.mi.ingv.it/ - Fragility Curves for Bridges o Research: Moschonas <i>et al.</i> ¹³ o URL: https://doi.org/10.1007/s10518-008-9077-2 (Access provided by CARE COMPACT-CRUI) - Landslide Hazard o Institution: Istituto Superiore per la Protezione e la Ricerca Ambientale (ISPRA) o City/Town/Region: Turin, Piedmont o Country: Italy o URL: https://idrogeo.isprambiente.it/app/iffi?@= - Fragility Curves for Buildings o Research: Rosti <i>et al.</i> ^{11,12} o URL: https://doi.org/10.1007/s10518-020-00971-4 ; (Open Access article) o https://doi.org/10.1007/s10518-020-00845-9 (Access provided by CARE COMPACT-CRUI) |

Table 4. Specification table of the data described in this document and reported in the open access directory.

Based on the values reported in Table 1, Miano *et al.*¹⁰ considered the values of PGA_c of reinforced concrete buildings using DS3 for the SLV condition while applying an average between DS1 and DS2 for the SLD condition. Then, by comparing PGA_c with PGA_d , both obtained by the random distributions described by Miano *et al.*^{10,27}, it is possible to assess the response of structures along the paths and determine their likelihood of failure.

It is noteworthy that, in addition to earthquakes, landslides are also prevalent in Italy²⁹, and several studies have investigated their impacts on the population³⁰. Thus, regarding landslides, the surveyed data concerning topography and soil parameters is provided in this dataset, as well as the relevant Safety Factor (SF) and critical acceleration³¹. Note that research in this field is ongoing, and a specific methodology to assess the resilience of networks under earthquake-induced landslides has yet to be validated. However, the domain of the dataset presented in this paper has already been validated. This ongoing research focuses on the impact of landslides on road networks, considering different saturation scenarios, and includes the impact of soil water content on slope stability. A saturation parameter is varied between 0 (dry conditions) and 1 (fully saturated) to represent best- and worst-case scenarios. Newmark displacement's method is then used to model slope behavior under seismic conditions, incorporating acceleration-time histories and critical acceleration to estimate the displacement of landslides along the road network. Further details can be found in Louagie *et al.*³².

Data Records

As mentioned, the dataset¹⁵ provides data regarding road networks and points of interest for the Turin and Naples case studies. Then, for each case study, the dataset identifies specific paths along the road networks that effectively connect the points of interest, and along these specific paths, buildings, bridges, and tunnels are individualized. The case study for Turin also identifies landslides that could interfere with the road networks and the analyzed paths.

The dataset is organized into shapefiles and spreadsheets to represent both the spatial dimension of the data and to facilitate an adequate understanding of calculations and parameters. To complement the data, original documentation, retrieved and collected on site by the Authors for the Turin case study, has been included to provide further information on the dataset components. This way, in the repository, the reader will find three main folders with the following structure and contents:

- Shapefiles (folder):
 - Naples (folder):
 - Bridges_Nap (shapefile folder)
 - Buildings_Nap (shapefile folder)



Fig. 8 Site surveying of bridge labelled as ‘11 F’ by Turin Municipality.



Fig. 9 Site surveying of the bridge labelled as ‘11D’ by Turin Municipality.

- Paths_Nap (shapefile folder)
- Points_Interest_Nap (shapefile folder)
- 00_Naples_Data (QGIS project)
- Turin (folder):
 - Bridges_Tunnels_To (shapefile folder)
 - Buildings_To (shapefile folder)
 - Landslides_To (shapefile folder)
 - Points_Interest_To (shapefile folder)
 - Road_Network_To (shapefile folder)
 - 00_Turin_Data (QGIS project)

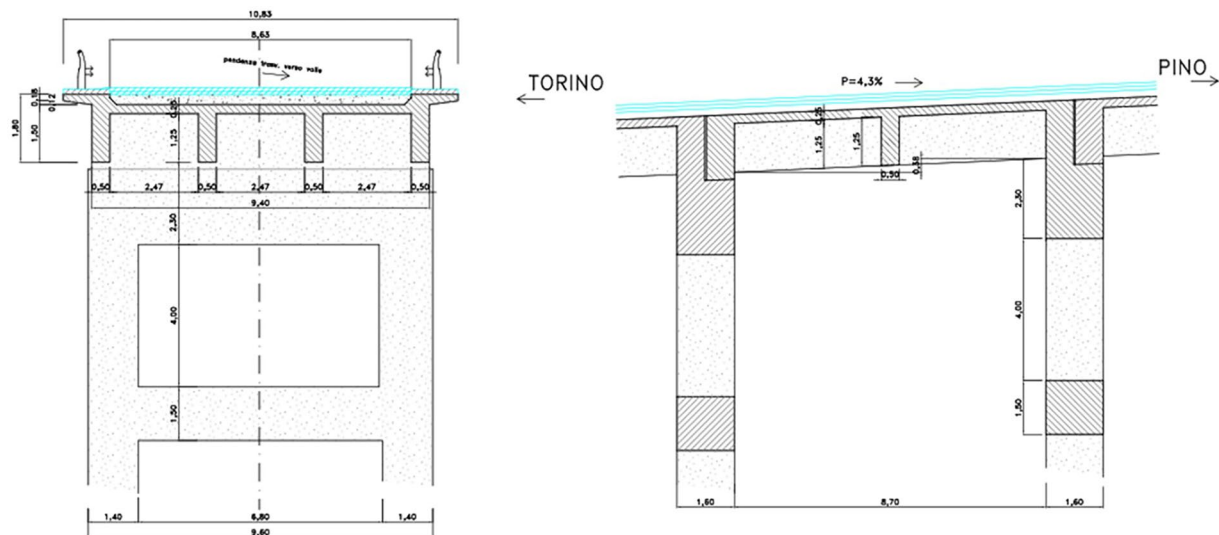


Fig. 10 Typical transversal and longitudinal section views from the retrieved documentation of a bridge along the selected paths of SS10 in Turin. All dimensions are in [m].

- Spreadsheets (folder):
 - Buildings&Bridges.xlsx
 - Landslides_data.xlsx
- Documentation (folder):
 - Bridge_images (folder)
 - Other_documents (folder)
 - 09-12-1949 lettera inizio lavori progettazione.pdf (data about tunnel included in the Turin section)
 - Modello_SVR.pdf (traffic information for the Turin road network)

Shapefiles. As indicated in the previous section, geospatial data are organized into two main groups: Turin data and Naples data.

The geospatial data described for Turin considers the five layers listed in Table 2, all of which use EPSG:32632 - WGS 84 / UTM zone 32 N as their coordinate reference system. On the other hand, geospatial data described for Naples considers the four layers listed in Table 3, all of which use EPSG:32633 - WGS 84 / UTM zone 33 N as their coordinate reference system.

Figs. 4 and 5 show a first approach to the geospatial representation of the data described for Turin, where it is possible to observe:

- Turin road network in Fig. 4, where the selected paths for the case study are highlighted in different colors, whereas those road network elements that are not part of the chosen paths have a light red color with a thinner line.
- Landslides are depicted in Fig. 4 as brown polygons, indicating the identified areas for each potentially hazardous element.
- Bridges and tunnels are shown in Fig. 4 within the selected paths in a cyan color.
- Points of interest are visible in Fig. 4 as red dots in the location of the hospitals that are of interest for the case study.
- Buildings, on the other hand, are more clearly visible in Fig. 5 as polygons along the selected paths.

A detailed description of the shapefiles described for the Turin case is presented in Table 2, where it is possible to observe the name of the layer, the type of geometry, the number of features (number of elements contained in each layer), a description, and, finally, the attributes assigned to the layer. Note that the attribute names reported in Table 2 specifically reflect the order of the attribute columns in the relevant shapefile.

Similar to what was exposed for the Turin case study, Figs. 6 and 7 show a general view of the geospatial data put together for the Naples case, where it is possible to observe:

- Paths selected for the hospital-to-hospital connection in Fig. 6, depicted in different colors.
- Bridges and overpasses are visible in Fig. 6, represented with a cyan color on top of the paths.
- Points of interest are shown in Fig. 6 as red dots in the location of the hospitals that are of interest for the case study.
- Buildings, on the other hand, are more clearly visible in Fig. 7 as polygons along the selected paths.

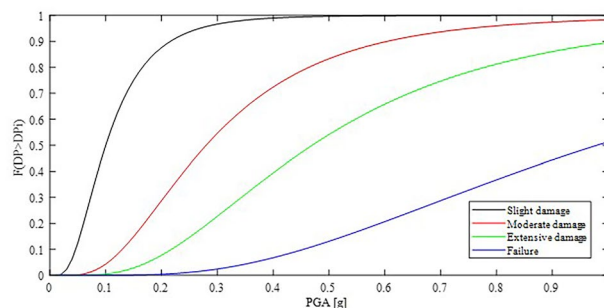


Fig. 11 Fragility curves for Siatista bridge¹³.

A detailed description of the shapefiles for the Naples case study is presented in Table 3, which contains the name of the layer, the type of geometry, the number of features (number of elements contained in each layer), a description, and finally the attributes assigned to each one.

Structures spreadsheets. The spreadsheets provided in the dataset¹⁵ are organized in an Excel file with eleven sheets. Sheets #1 - #4 and sheets #6 - #10 include information on buildings adjacent to the different paths that were the subject of this study in Turin and Naples, respectively. In these sheets, the following information can be found:

- **Column A:** OID (object identifier) of each building, and in case this value is missing, **column B** reports the ISTAT number associated with the area where the building is found.
- **Column C:** height of the building.
- **Column D:** year of construction.
- **Column E:** number of stories.
- **Column F:** type of construction material, which is classified as either reinforced concrete (“RC”) or unreinforced masonry (“masonry”).
- **Column G:** layer in QGIS where the information about the buildings can be found.

For assessing the PGA of buildings, the dataset utilizes fragility curves developed from previous literature, as explained in the next section. Please note that all values of PGA are expressed in terms of g , i.e., 9.81 m/s^2 .

- **Column I:** median of the PGA distribution for the damage state associated with ultimate limit state (“SLV”, i.e., Stato Limite di salvaguardia della Vita), which indicates pending structural failure with loss of user safety, in g .
- **Column K:** median of the PGA distribution for the damage state associated with serviceability limit state (“SLD”, i.e., Stato Limite di Danno), where structural functionality, such as comfort and minor deformations, is affected without immediate structural risk, in g .

In the dataset, from columns O to V, the data in each row categorizes buildings’ limit states based on different characteristics:

- **Column O:** construction date (pre- or post-1981).
- **Column P:** height classification: low (1–2 stories), medium (3–4 stories), and high rise (more than four stories).
- **Columns Q to U:** medians of the PGA distributions for different damage states associated with buildings based on the two attributes stated before.

For each building, the following is also reported:

- **Column J, Column L:** the corresponding standard deviation for the PGA distributions.

In the fifth and eleventh sheets, data regarding bridges and viaducts are provided, obtained after a preliminary site survey and satellite-supported analysis to characterize these structures. For the fragility assessment of bridges, this study relies on the work of Moschonas *et al.*¹³, and the sheets are organized in the following way:

- **Column C:** contains the bridge identification code, which is a naming convention defined by the study as reported in the main article.
- **Column D:** provides a brief description of each bridge.
- **Column E:** median of the PGA distribution for the damage state associated with ultimate limit state (“SLV”, i.e., ‘Stato Limite di salvaguardia della Vita’ in Italian language), in g .
- **Column F:** standard deviation values for ultimate limit state thresholds, in g .

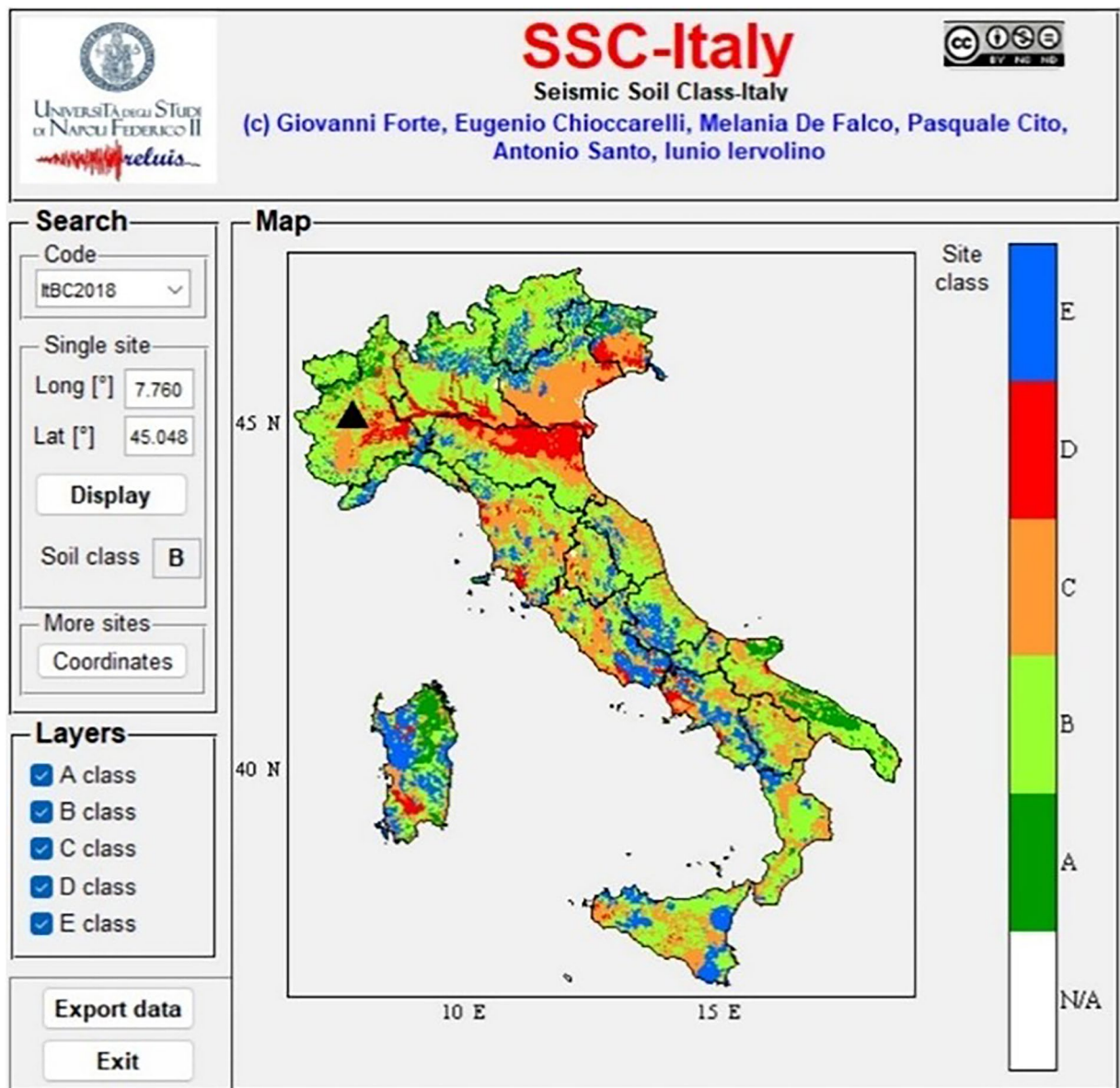


Fig. 12 Outcomes of SSC-Italy for the example coordinates.

- **Column G:** median of the PGA distribution for the damage state associated with serviceability limit state ("SLD" i.e. 'Stato Limite di Danno'), in g.
- **Column H:** standard deviation values for serviceability limit state thresholds, in g.
- **Column I:** number of spans of the bridge.

Landslide spreadsheets. The spreadsheets with landslide data for the Turin case study provided in the dataset¹⁵ are organized according to the paths into a four-sheet Excel file, where each sheet describes all the landslides that represent a threat to one of the paths. For this, the sheets are organized as follows:

- **Column A:** landslide identification number.
- **Step 1** (columns B to E): Parameters for slope angle determination:
 - **Column B:** height of the top (H2), maximum height of the probable failure surface, in meters.
 - **Column C:** height of the foot (H1), starting height of the probable failure surface, in meters.
 - **Column D:** horizontal distance between H1 and H2, horizontal distance between the starting point and the maximum height of slip surface, in meters.
 - **Column E:** slope angle of the slip surface, in sexagesimal degrees.
- **Step 2** (Columns F to I): soil parameters for mechanic response estimation:
 - **Column F:** effective friction angle of the soil, in sexagesimal degrees.

- **Column G:** effective cohesion of the soil, in kPa.
- **Column H:** volumetric weight of the soil, in kN/m³.
- **Column I:** Peak Ground Acceleration (PGA), in g.
- **Step 3** (Columns J to M): SF and critical acceleration for both dry and fully saturated conditions:
 - **Column J:** SF for $m = 0$.
 - **Column K:** a_c for $m = 0$.
 - **Column L:** SF for $m = 1$.
 - **Column M:** a_c for $m = 1$.

Additional specifications. In conclusion, additional specifications, recalling the data description reported in the previous parts of this section, are summarized in Table 4. All data can be downloaded in open access from the reported URLs.

Technical Validation

This section discusses the technical validation, value of the data, and the dataset limitations. The value of the dataset¹⁵ lies in its ability to provide integrated, geo-referenced, and site-specific data that bridges the gap between single-structure assessments and network-level resilience evaluation.

The dataset addresses seismic hazard by considering demand peak ground acceleration based on the location of the structures and seismic vulnerability, relating the structures' fragility curves to different values of capacity peak ground acceleration. To evaluate road network disruptions caused by multiple hazards, the dataset also incorporates landslide hazards based on their location.

The data provide inputs for the seismic and post-event efficiency assessment of urban road networks through Monte Carlo simulations. Specifically, the data address the infrastructure capital of two case studies. The first one is a rural road network connecting the two towns of Pino Torinese and Chieri to a hospital located in Turin, Italy. The second one is an urban road network connecting two hospitals in Naples, Italy.

Furthermore, the included output data provides starting points for researchers in the same area to build upon or calibrate against. They can be of value for researchers working on the topic of infrastructural risk assessment and seismic hazards through the application of GIS-based maps.

To summarize, this dataset can be utilized by researchers and policymakers, who would benefit from information gathered through expert-based on-site and online surveys. These surveys concerned the structural health and seismic vulnerability of roads, bridges, and buildings within the associated road networks.

We acknowledge some limitations of the current dataset, as some of the provided data was not always directly available in the cited sources, and thus:

- The number of floors of buildings was not always available, and when needed, it was estimated using satellite services (Google Earth and Google Street View).
- The number of stories was used instead of the building height to evaluate the seismic fragility as it provides a practical proxy for a building's dynamic response during seismic events. However, this simplification may introduce uncertainties in cases where story heights vary significantly.
- The construction period of the building was not always available; in those cases, the worst conditions were considered (pre-1981).
- Building material was not always available; in such cases, reinforced concrete has been applied.

Additionally, to retrieve the values of PGA_d for buildings, bridges, and landslides, the analysis consisted in applying a uniform PGA value across the region, derived from grid-based seismic hazard estimation using the model MPS04 from the Istituto Nazionale di Geofisica e Vulcanologia (INGV)¹⁸. This approach may overlook localized differences in ground motion amplification.

According to the Italian building code (Norme Tecniche per le Costruzioni, Chapter 3.2.3 'Evaluation of the seismic action'), the PGA values, calculated for a reference rigid and flat surface, should be locally amplified/deamplified in accordance with the local stratigraphy and topography.

As an example, the point of coordinates (45°02'52.8"N; 7°45'36.0"E), situated along the purple path in Fig. 1, is analyzed. The uncorrected PGA equals 0.050 g (for an annual frequency of exceedance 0.0021, i.e., 10% probability in 50 years).

Stratigraphically, the local soil can be estimated thanks to the SSC-Italy software. An example screenshot of the software is shown in Fig. 12; the software is available at <http://wpag.unina.it/iuniervo/SSC-Italy.zip> and described in Forte *et al.*³³; in this case, the site falls in the category B (According to NTC 2018: Table 3.2.II: "deposits of very dense sand, gravel, or very stiff clay, at least several tens of meters in thickness, characterized by a gradual increase of mechanical properties with depth").

Thus, the corresponding amplification factors should be computed as

$$S_s = 1.00 < 1.40 - 0.40 \cdot F_0 \cdot \frac{PGA}{g} \leq 1.20 \quad (1)$$

according to NTC 2018: Table 3.2.IV. Similarly, the maximum spectral amplification F_0 can be estimated according to what is prescribed in NTC2018 § 3.2.3.2.1, obtaining here $F_0 = 2.2$. Based on that, one obtains $S_s = 1.40$ (upper limited to 1.20).

Topographically, this is a situated along a hill crest where the average hill slope does not exceed 30 degrees. Hence, the Topographic category is T3 and the Amplification Factor is equal to $St = 1.2$ (NTC 2018: Table 3.2.V). Combining the two corrective factors, one has $PGA \cdot S_s \cdot S_p$, which here returns 0.072 g (instead of 0.050 g).

Finally, we highlight that, despite several attempts by the authors to communicate with the local authorities, access to any detailed information regarding the Traforo del Pino tunnel was not granted.

Code availability

No custom code beyond standard MATLAB/QGIS functions was used to generate or process the data described in this manuscript.

Received: 9 April 2025; Accepted: 29 August 2025;

Published online: 03 October 2025

References

- Hong, B., Bonczak, B. J., Gupta, A. & Kontokosta, C. E. Measuring inequality in community resilience to natural disasters using large-scale mobility data. *Nat Commun* **12**, 1870 (2021).
- Opabola, E. A. & Galasso, C. Informing disaster-risk management policies for education infrastructure using scenario-based recovery analyses. *Nat Commun* **15**, 325 (2024).
- Blagojević, N., Hefti, F., Henken, J., Didier, M. & Stojadinović, B. Quantifying disaster resilience of a community with interdependent civil infrastructure systems. *Structure and Infrastructure Engineering* **19**, 1696–1710 (2023).
- Opabola, E. A. & Galasso, C. A probabilistic framework for post-disaster recovery modeling of buildings and electric power networks in developing countries. *Reliab Eng Syst Saf* **242**, 109679 (2024).
- Cimellaro, G. P., Solari, D. & Bruneau, M. Physical infrastructure interdependency and regional resilience index after the 2011 Tohoku Earthquake in Japan. *Earthq Eng Struct Dyn* **43**, 1763–1784 (2014).
- Argyroudis, S. A. *et al.* Resilience assessment framework for critical infrastructure in a multi-hazard environment: Case study on transport assets. *Science of The Total Environment* **714**, 136854 (2020).
- Capacci, L., Biondini, F. & Frangopol, D. M. Resilience of aging structures and infrastructure systems with emphasis on seismic resilience of bridges and road networks: Review. *Resilient Cities and Structures* **1**, 23–41 (2022).
- Byun, J.-E. & D'Ayala, D. Urban seismic resilience mapping: a transportation network in Istanbul. *Turkey. Sci Rep* **12**, 8188 (2022).
- Wu, Y., Hou, G. & Chen, S. Post-earthquake resilience assessment and long-term restoration prioritization of transportation network. *Reliab Eng Syst Saf* **211**, 107612 (2021).
- Miano, A. *et al.* Efficiency Assessment of Urban Road Networks Connecting Critical Node Pairs under Seismic Hazard. *Sustainability* **16**, 7465 (2024).
- Rosti, A., Rota, M. & Penna, A. Empirical fragility curves for Italian URM buildings. *Bulletin of Earthquake Engineering* **19**, 3057–3076 (2021).
- Rosti, A. *et al.* Empirical fragility curves for Italian residential RC buildings. *Bulletin of Earthquake Engineering* **19**, 3165–3183 (2021).
- Moschonas, I. F. *et al.* Seismic fragility curves for greek bridges: methodology and case studies. *Bulletin of Earthquake Engineering* **7**, 439–468 (2009).
- Cardone, D., Perrone, G. & Sofia, S. A performance-based adaptive methodology for the seismic evaluation of multi-span simply supported deck bridges. *Bulletin of Earthquake Engineering* **9**, 1463–1498 (2011).
- Aloschi, F. *et al.* Seismic resilience of urban networks: dataset for infrastructure visualization and vulnerability assessment. *Figshare*, <https://doi.org/10.6084/m9.figshare.28733174>.
- Sterlacchini, S., Bordogna, G., Cappellini, G. & Voltolina, D. SIRENE: A Spatial Data Infrastructure to Enhance Communities' Resilience to Disaster-Related Emergency. *International Journal of Disaster Risk Science* **9**, 129–142 (2018).
- QGIS Development Team. QGIS Geographic Information System. Open Source Geospatial Foundation Project. <http://qgis.osgeo.org> (2025).
- Stucchi, M. *et al.* Seismic Hazard Assessment (2003–2009) for the Italian Building Code. *Bulletin of the Seismological Society of America* **101**, 1885–1911 (2011).
- ISPRA. Istituto Superiore per la Protezione e la Ricerca Ambientale. <https://www.isprambiente.gov.it/it> (2025).
- Direzione Ambiente Energia e Territorio. Regione Piemonte, GeoPortale Piemonte. <https://geoportale.igr.piemonte.it/cms/> (2025).
- Sistema Informativo Territoriale (SIT). Geoportale Regione Campania. <https://sit2.regione.campania.it/node> (2025).
- Crowley, H. *et al.* A comparison of seismic risk maps for Italy. *Bulletin of Earthquake Engineering* **7**, 149–180 (2009).
- Kircher, C. A., Whitman, R. V. & Holmes, W. T. HAZUS Earthquake Loss Estimation Methods. *Nat Hazards Rev* **7**, 45–59 (2006).
- Li, X. *et al.* Seismic vulnerability comparison between rural Weinan and other rural areas in Western China. *International Journal of Disaster Risk Reduction* **48**, 101576 (2020).
- Crowley, H. *et al.* Exposure model for European seismic risk assessment. *Earthquake Spectra* **36**, 252–273 (2020).
- Aloschi, F. *et al.* A seismic vulnerability model for masonry buildings in Montenegro. *Bulletin of Earthquake Engineering* **23**, 2347–2376 (2025).
- Miano, A. *et al.* A framework for the assessment of road network resilience: application to a densely populated urban context. *Procedia Structural Integrity* **64**, 311–318 (2024).
- Nielson, B. G. Analytical Fragility Curves for Highway Bridges in Moderate Seismic Zones (2005).
- Guzzetti, F. Landslide fatalities and the evaluation of landslide risk in Italy. *Eng Geol* **58**, 89–107 (2000).
- Guzzetti, F., Stark, C. P. & Salvati, P. Evaluation of Flood and Landslide Risk to the Population of Italy. *Environ Manage* **36**, 15–36 (2005).
- Niño, M., Jaimes, M. A. & Reinoso, E. Seismic-event-based methodology to obtain earthquake-induced translational landslide regional hazard maps. *Natural Hazards* **73**, 1697–1713 (2014).
- Louagie, M. *et al.* A framework for assessing the earthquake-induced landslide resilience of a road network in Turin, Italy. in *10th ECCOMAS Thematic Conference on Computational Methods in Structural Dynamics and Earthquake Engineering (COMPADYN 2025)* (Rhodes, 2025).
- Forte, G. *et al.* Seismic soil classification of Italy based on surface geology and shear-wave velocity measurements. *Soil Dynamics and Earthquake Engineering* **122**, 79–93 (2019).

Acknowledgements

The authors acknowledge the financial support of projects PE3 RETURN, Spoke: TS2 - MULTI-RISK RESILIENCE OF CRITICAL INFRASTRUCTURES. MUR project code: PE00000005 and MOST - Sustainable Mobility National Research Center - SPOKE 7 “Cooperative Connected and Automated Mobility and Smart Infrastructures” - WP4”. Moreover, the authors wish to acknowledge Mr. Filippo Dringoli, Mr. Davide Petralia,

Mr. Maxim Louagie, Mr. Cesare Cilvini, Mr. Antonino Fiorentino, and especially Mr. Amirmoahamad Parvanehdehkordi for their support in the earliest stages of this dataset collection. The Ufficio Ponti of the Comune di Torino is also acknowledged for its support and for providing extensive information on the bridges under its jurisdiction.

Author contributions

Marco Civera: Conceptualization, Data curation, Writing - Original draft preparation, Methodology. Fabrizio Aloschi: Conceptualization, Data curation, Writing - Original draft preparation, Methodology, Software. Galilea Margherita Di Maio: Data curation, Writing - Review. Juan Pablo Fierro Carrasco: Data curation, Writing - Review. Andrea Miano: Methodology. Bernardino Chiaia: Supervision. Andrea Prota: Supervision. All authors have approved the final version of the manuscript.

Competing interests

The authors declare that they have no known competing financial interests or personal relationships that could have appeared to influence the work reported in this paper.

Additional information

Correspondence and requests for materials should be addressed to F.A.

Reprints and permissions information is available at www.nature.com/reprints.

Publisher's note Springer Nature remains neutral with regard to jurisdictional claims in published maps and institutional affiliations.



Open Access This article is licensed under a Creative Commons Attribution-NonCommercial-NoDerivatives 4.0 International License, which permits any non-commercial use, sharing, distribution and reproduction in any medium or format, as long as you give appropriate credit to the original author(s) and the source, provide a link to the Creative Commons licence, and indicate if you modified the licensed material. You do not have permission under this licence to share adapted material derived from this article or parts of it. The images or other third party material in this article are included in the article's Creative Commons licence, unless indicated otherwise in a credit line to the material. If material is not included in the article's Creative Commons licence and your intended use is not permitted by statutory regulation or exceeds the permitted use, you will need to obtain permission directly from the copyright holder. To view a copy of this licence, visit <http://creativecommons.org/licenses/by-nc-nd/4.0/>.

© The Author(s) 2025